The Enhancement of Microvoids in Acrylic Fibers

JIAN QIN*

Man-Made Fiber Research Association, China Textile University, Shanghai, People's Republic of China

SYNOPSIS

The present work is concerned with the spinning of two series of blend fibers containing acrylic copolymer (PAC) and small amount of secondary polymer, such as polyvinyl acetate (PVAc), polystyrene (PS), acrylonitrile–styrene (AS) and acrylonitrile-vinyl acetate (AVAc) copolymers. The blend acrylic fibers we developed have a microporous structure that renders them highly water retentive and confers several other excellent properties. Some factors were further studied that greatly influence the microporous volume and micropore size distribution, such as compatibility and phase separation of the polymer blends, the composition and sequence distribution of the secondary copolymers, and fiber formation conditions.

INTRODUCTION

While in the case of normal polyacrylonitrile copolymer fibers, the presence of voids is usually looked upon as a defect, in special cases it becomes an advantage by imparting to the acrylic fibers high water-retentive, excellent diffusion, and heat-insulating properties.

Early porous acrylic fibers were produced by some novel methods, like adding some soluble material into the fibers during formation processes and then removing it by a washing after-treatment. Such methods were inefficient and expensive.[1]

During the past decade, much technical and scientific information concerning acrylic blends appeared in the literature that opened the way to the successful commercial production of highly water-retentive acrylic fibers of much practical value.[2–4]

The application of highly water-retentive acrylic fibers is chiefly in the fields of sportswear, swimming suits, and dressing materials of excellent drying, dyeing, and warmth-retentive properties. They exceed regular acrylic, other synthetic fibers, and even cotton in these respects, which give rise to better wear comfort.

EXPERIMENTAL

Polyacrylonitrile and its copolymers (PAC) were prepared using a conventional polymerization technique. The acrylonitrile content in the copolymers was measured by pyrolytic chromatography. The PAC copolymer was made up of acrylonitrile (90.9%), methyl acrylate (8.6%), and sodium methyl propenyl sulfonate (0.5%) with molecular weight of 72,000.

The PAC and the copolymers were blended and dissolved into dimethylformamide (DMF) as 20% dopes. The dopes were extruded from a 48-hole (0.08 mm diameter) die into a 55% DMF aqueous coagulation bath at 25°C to form the fibers, which were then washed, drawn in a boiling water bath, and dried at 110°C for 2 hs.

Phase-contrast microscope was used to study the phase morphology of the PAC/AS blend films as well as their solutions. The films for observation were about 0.1 mm thick and held on the slide.

IR spectra of acrylonitrile–styrene (AS) copolymers were recorded on a Perkin-Elmer 599 spectrophotometer. Samples were prepared by pressing their solution in DMF into 0.1-mm-thick films. In

---

order to measure accurate frequency shifts, IR measurements were made using 20 times the abscissa expansion at a 10 cm^{-1}/min scanning rate.

The cross-sectional and surface morphologies of the fibers, after freezing and breaking in liquid N_2 and then spraying with gold, was observed using a JSM-35 SEM. The films of AS polymer blends were cast from a DMF solution, immersed in butanone for 12 h to remove the AS component or coagulated in water, washed, and dried in a vacuum oven at 40°C. Sprayed with gold, the films were then photographed with a TSM-1 SEM.

The microvoid distribution in the fibers was measured with a J5-70 mercury porosimeter. The mercury pressure changed from 1 to 2500 atm.

The immersion density of the fibers was measured in a wetting mixture of carbon tetrachloride and toluene. The mercury density of the fibers was measured by the simple volume method[5] that uses mercury to replace the wetting mixture and measures at very high vacuum.

To measure the water retention (WR) of the samples, about 0.5 g of fiber was immersed in water for 1 h and then dewatered for 1 h by means of a centrifugal hydroextractor that could produce 1000G gravitational acceleration (G = 9.8 m/s^2).

PRINCIPLE AND PRACTICE OF DEVELOPING VOID STRUCTURE IN ACRYLIC FIBERS

Notation Usually Used in Polymer Blends

At present, a majority of varieties of the commercial porous acrylic fibers are produced by blending the dope used for producing regular polyacrylonitrile copolymer fiber (designated here as polymer 1) with a certain amount of a second polymer (polymer 2) composed generally of a copolymer of acrylonitrile with another monomer like styrene (S) or vinyl acetate (VAc). The composition of the polymer 2 is usually expressed as AN/S (or AN/VAc) in proportion 55/45 wt %, etc. The blend ratio is written as PAC/AS (or PAC/AVAc), for example, 90/10, also in wt %; when the acrylonitrile content in polymer 2 is zero, AS or AVAc then become PS or PVAc. [Strictly speaking, AS or AVAc here should be written as PAS or PAVAc.]
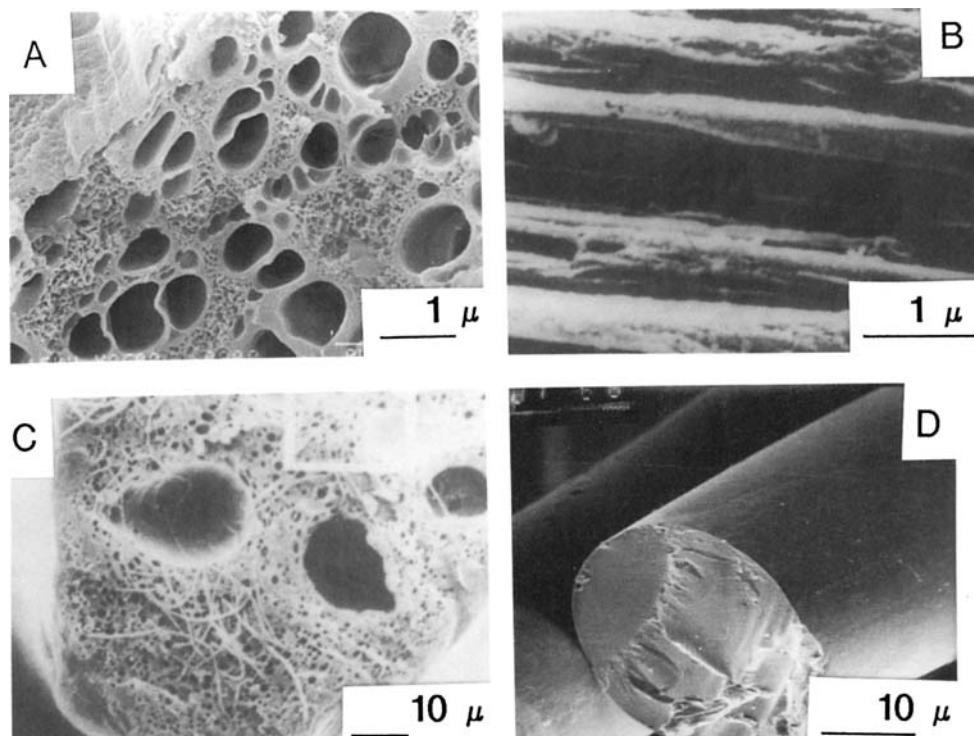

Figure 1   The electron micrographs of the blend acrylic fibers: (a) Cross section of the blend fiber, (b) surface morphology of the blend fiber, (c) micropores on interphase region of two polymers, and (d) normal acrylic fiber.

Compatibility of the Polymers in the Blends

Incompatibility and phase separation is an indispensable requisite for water retention. A necessary condition for producing porous, water-retentive acrylic fibers is that polymers 1 and 2 in the blend must be incompatible whether in solution or in fibers and films.

When an acrylic fiber is formed from a dope consisting of a blend of two incompatible polymers and the content of polymer 2 exceeds a certain critical amount, phase separation will occur in the resulting fiber, yielding void spaces in the fiber. Figure 1 shows the general morphological characteristics of a typical porous acrylic blend fiber, under an electron microscope, showing the cross section, longitudinal section, and the surface appearance.

The site of absorption of water in the fiber is mostly in the interphase regions, although in one or both phases a system of small voids must be present that constitute capillary conduits for transferring water in or out of the fiber.

Theoretical Prediction of Compatibility and Phase Separation

From Flory–Huggins solution theory, it can be deduced that the compatibility of two polymers A and B in a blend can be related to the difference of their respective solubility parameters ($\Delta\delta = \delta_A - \delta_B$). Scott[6] suggested that for a bicomponent blend a thermodynamic criterion for incompatibility or phase separation is judged by

$$\Delta\delta \leq 3.3\,(RT\rho/2M_w)^{1/2} \qquad (1)$$

in which ρ and M_w are the density and molecular weight of the polymer sample concerned. For $\rho = 1$ and $M_w = 100{,}000$, roughly, $\Delta\delta$ is 0.18, above which phase separation is unavoidable.

The value of solubility parameter for a copolymer δ_C can be calculated from

$$\delta_c = \sum \delta_i \phi_i \qquad (2)$$

where δ_i is the solubility parameter of a homopolymer composed of a monomer existing in the copolymer concerned, and the summation is taken over all the monomers in the copolymer.

Using Scott's Eqs. (1) and (2), prediction of phase separation can be calculated, using 12.4, 9.48, 9.05, and 9.70 $(cal/cm^3)^{1/2}$ as the values of polyacrylonitrile (PAN), polyvinyl acetate (PVAc),

Table I Prediction of Phase Separation in Polymer Blends by Scott Equation

Polymer	Composition (wt %)	ϕ_1 (mol %)	ϕ_2 (mol %)	δ_c $(cal/cm^3)^{1/2}$	$\Delta\delta^a$	Phase Separation
PAC	AN : MA : MAS (90.9 : 8.6 : 0.5)	94.19	5.18	12.53		
PAN	AN (100)	100	0	12.70	0.17	No (< 0.18)
AS1	AN : S(84.25 : 15.75)	91.30	8.70	12.38	0.15	No (< 0.18)
AS2	AN : S(75.64 : 24.36)	85.90	14.10	12.18	0.35	Yes (> 0.18)
AS3	AN : S(54.66 : 45.34)	70.29	29.71	11.62	0.91	Yes (> 0.18)
AS4	AN : S(49.71 : 50.29)	65.98	34.02	11.46	1.07	Yes (> 0.18)
AS5	AN : S(45.64 : 54.36)	62.23	37.77	11.32	1.21	Yes (> 0.18)
AS6	AN : S(40.41 : 59.59)	57.09	42.91	11.13	1.40	Yes (> 0.18)
AS7	AN : S(34.05 : 65.95)	50.33	49.67	10.89	1.64	Yes (> 0.18)
AS8	AN : S(28.52 : 71.48)	43.91	56.09	10.65	1.88	Yes (> 0.18)
AS9	AN : S(20.25 : 79.75)	33.26	66.74	10.26	2.27	Yes (> 0.18)
AS10	AN : S(11.41 : 88.59)	20.17	79.83	9.79	2.74	Yes (> 0.18)
PS	S (100)	0	100	9.05	3.48	Yes (> 0.18)
AVAc1	AN : VAc(87.6 : 12.4)	91.98	8.02	12.44	0.09	No (< 0.18)
AVAc2	AN : VAc(80.3 : 19.7)	86.87	13.13	12.28	0.25	Yes (> 0.18)
AVAc3	AN : VAc(70.9 : 29.1)	79.85	20.15	12.05	0.48	Yes (> 0.18)
AVAc4	AN : VAc(43.6 : 56.4)	55.64	44.36	11.27	1.26	Yes (> 0.18)
AVAc5	AN : VAc(38.9 : 61.1)	50.81	49.19	11.12	1.41	Yes (> 0.18)
PVAc	VAc(100)	0	100	9.48	3.05	Yes (> 0.18)

$^a \Delta\delta = \delta_{PAC} - \delta_c$.

polystyrene (PS), and polymethyl acrylate (PMA), respectively. The results so calculated are listed in Table I. From these it can be concluded that phase separation will occur for polyblend polymer pairs PAC/AS and PAC/AVAc when styrene content lies between 15.7 and 24.4 wt % and VAc content between 12.4 and 19.7 wt %.

Such phase separation occurs both in the dope and in the film formed from the dope. Optical micrographs of the dopes and films, by using phase contrast microscope, are shown in Figures 2 and 3. In Figure 2(a) for PAC/AS (50/50) blend film, with S content of 15.7%, phase separation can scarcely be observed. This is also true for the dope of the same blend and composition as shown in Figure 3(a). Above this S content from 24.36% up to 100%, phase separation always occurs. From these results it can be inferred that Scott's prediction of the phase separation as has already been described is valid and that phase separation is an inherent property of the dope and is not created by the coagulation process of the films.

Table II   Sequence Distribution Parameters of AS Copolymers

AN (mol %)	$f_{C=N}$ (cm^{-1})	P_{AN-AN}	R	$\langle AN \rangle$	$\langle S \rangle$
100	2239.6	1.00	0	100	0.00
85.90	2239.4	0.96	6.87	25.00	4.10
70.29	2238.6	0.84	22.49	6.25	2.64
62.23	2237.5	0.58	26.14	4.76	2.89
50.33	2235.5	0.18	41.27	2.44	2.41
33.26	2234.8	0.04	31.93	2.08	4.18
0	—	0.00	0	0	100

Relation between Sequence Distribution of Added Copolymer (Polymer 2) and Void Structure

The Sequence Distribution Parameters

The term *sequence* means a segment of copolymer chain composed of the one and the same monomer. For a bicomponent copolymer chain composed of
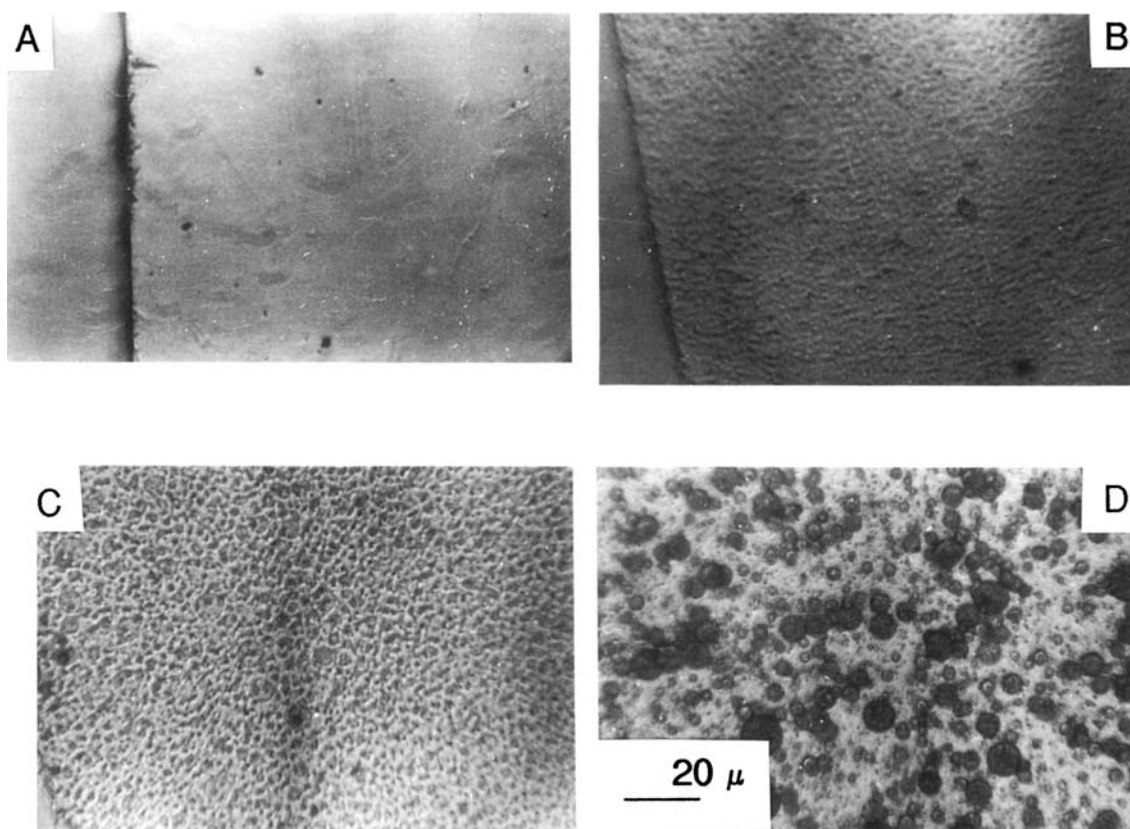

Figure 2   Phase separation of PAC/AS (50/50) blend films AN content in AS copolymer (wt %): (a) 84.25, (b) 75.64, (c) 45.64, and (d) 0.
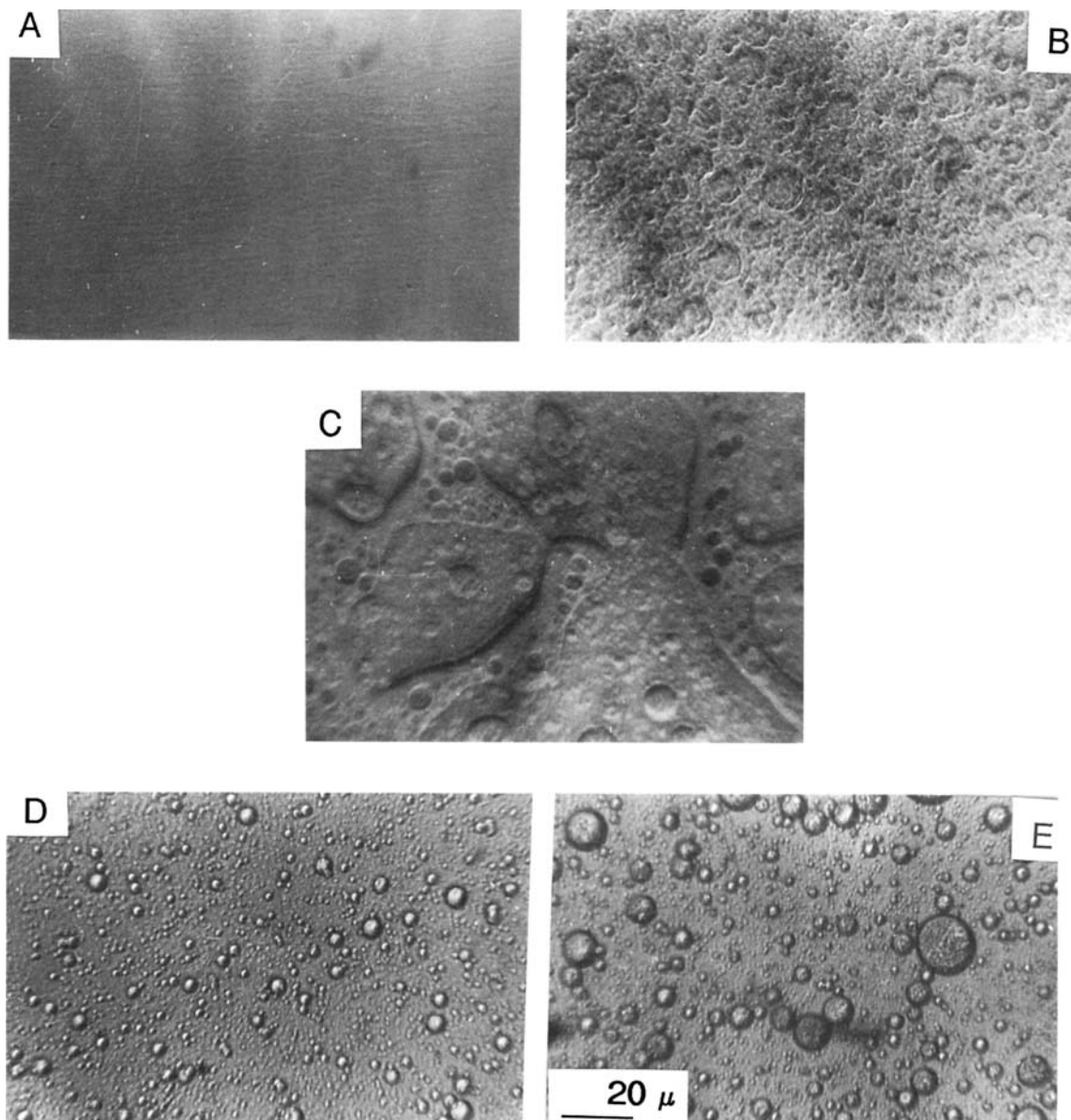
Figure 3 Phase separation of PAC/AS (50/50) blend dopes in DMF AN Content in AS copolymer (wt %): (a) 84.25, (b) 75.64, (c) 45.64, (d) 34.04, and (e) 0.

monomer A and monomer B, the number of –A–A—A– sequences and –B–B—B– sequences must be same and each equal to $R/2$, where R is the average number of monomer sequences occurring in a copolymer per 100 monomer units and is usually termed the "run number." Of course, for a random copolymer the different sequences are not of the same length, but a number-average sequence length can be calculated. For an AN/S or AN/VAc copolymer, these number-average sequence lengths are denoted as $\langle AN \rangle$ or $\langle S \rangle$. If the composition of the AN/S (or AN/VAc) copolymer (%AN and %S or %AN and %VAc) is known, the different sequence distribution parameters can be calculated from the following group of equations:

$$\langle AN \rangle = \%AN / R / 2 \qquad (3)$$

$$\langle S \rangle = \%S / R / 2 \qquad (4)$$

$$P_{AN\text{-}AN} = (\%AN - R/2)/\%AN \qquad (5)$$
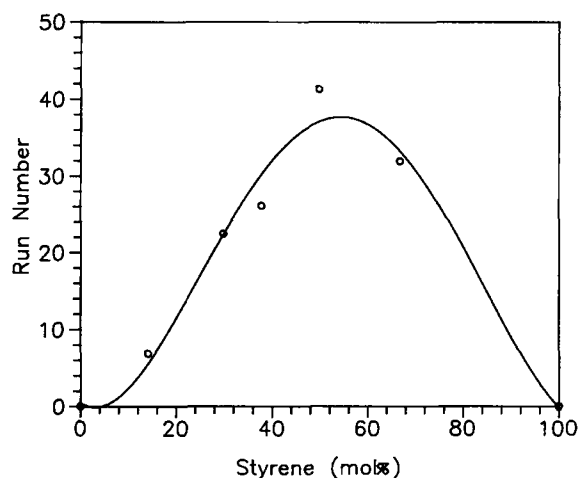
Figure 4 The run numbers related to the S content in the AS copolymers.

P_{AN-AN} in Eq. (5) is the probability of the AN–AN linkages, which can be calculated for the AS copolymer from the amount of frequency shift of the 2240 cm^{-1} C≡N line by IR spectroscopy. It was found[7]

that the probability of AN–AN linkages is linearly related to the C≡N stretching frequency and thus the former can be experimentally measured. With the P_{AN-AN} value so found, the sequence parameters R, $\langle AN \rangle$, and $\langle S \rangle$ can be calculated. The values are all listed in Table II and plotted in Figure 4.

From these results it can be seen that when the content of either monomer in the copolymer is low, the average number of sequences R in the macromolecule could be reasonably expected to be low too. The R value would reach a maximum when the AN and S (or VAc) values are each around 50 mol %.

The Effects of Sequence Distribution Parameters on the Structure of Blend Fibers

While compatibility and phase separation is a prerequisite to void structures, the details of the micro- and macrovoid structure are influenced greatly by the interaction of macromolecular chains of the two polymers that constitute the blend. For a PAC/AS or PAC/AVAc blend, the difference in properties between polymer 1 and 2 will be greater, the greater
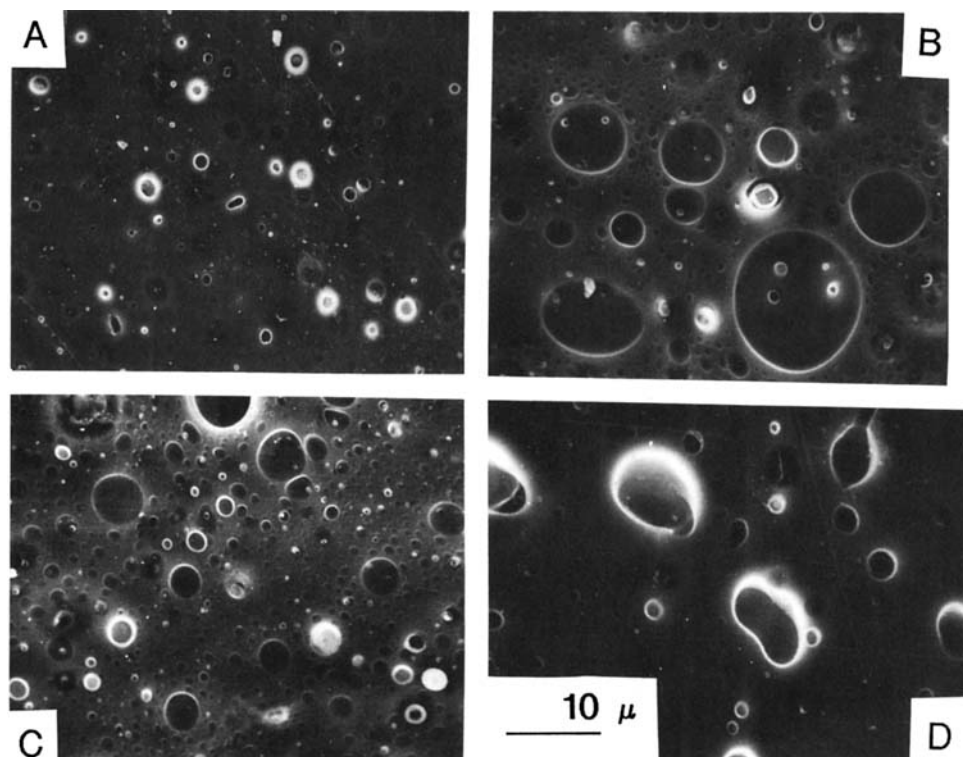

Figure 5 Electron micrographs of the PAC/AS (90/10) films treated with butanone AN content in AS copolymers (mol %): (a) 70.29, (b) 62.23, (c) 50.33, and (d) 0.
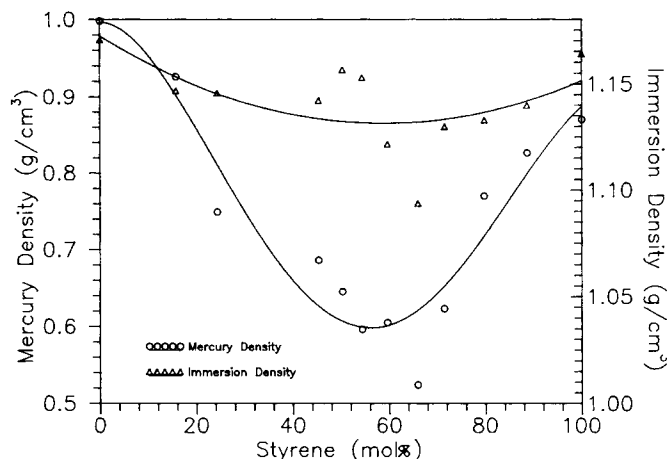
Figure 6 Effect of AS composition on densities of PAC/AS blend fibers.

is the content of styrene or vinyl acetate in the co-polymer (polymer 2) and the more evenly it is distributed in the copolymer macromolecule. These are the reasons why run number R and number-average sequence length $\langle AN \rangle$ or $\langle S \rangle$ can exert great influence on the structure of the blend fiber.

In the usual case of forming PAC–copolymer blend, the copolymer content is usually around 10%; when the styrene content is about 15%, the limit of incompatibility is reached. Further rise of S content will cause phase separation, and the higher the S content becomes, the coarser will be the resulting dispersion. At very high S content, the separated phase will agglomerate into fine droplets. Such phe-

nomena can be seen from the electron micrograph shown in Figure 5.

Beside by electron microscopy, the void structure of a porous PAC–copolymer fiber can be revealed by both immersion density (ρ) and mercury density (ρ_{Hg}). The multitudes of fine pores are accessible to the organic solvents used in immersion density determination, but not to mercury when it is used as the immersion medium because of the capillary depression of mercury. Thus the ρ_{Hg} of porous acrylic fiber may be as low as only a little above half of ρ. The difference between ρ and ρ_{Hg} is a measure of porosity of the porous fiber. The quantity void proportion (VP) can be written as
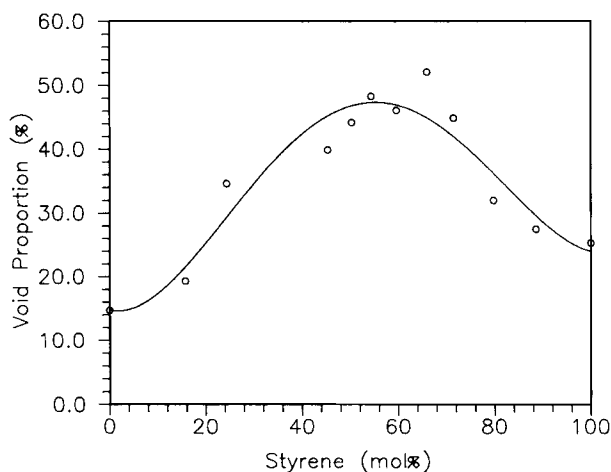
$$VP = (\rho - \rho_{Hg})/\rho \qquad (6)$$

Figures 6 and 7 illustrate the void structure of a PAC/AS (94/6) of a blend copolymer fiber. When the styrene content of the copolymer in the blend is around 60 wt % (about 50 mol %), both ρ and ρ_{Hg} of the blend fiber show minima and the VP shows a maximum. It should be noted that run number R also shows a maximum around 50 mol % styrene. So it is logical to expect a linear relationship between VP and run number, as is shown in Figure 8.

Void Structure as a System of Capillaries and Interphase Void Spaces

Figure 7 Effect of AS composition on VP of the PAC/AS blend fibers.

Although no large pear- or finger-shaped voids, like those sometimes appearing as a result of faults in the wet spinning of acrylic fibers, can be observed
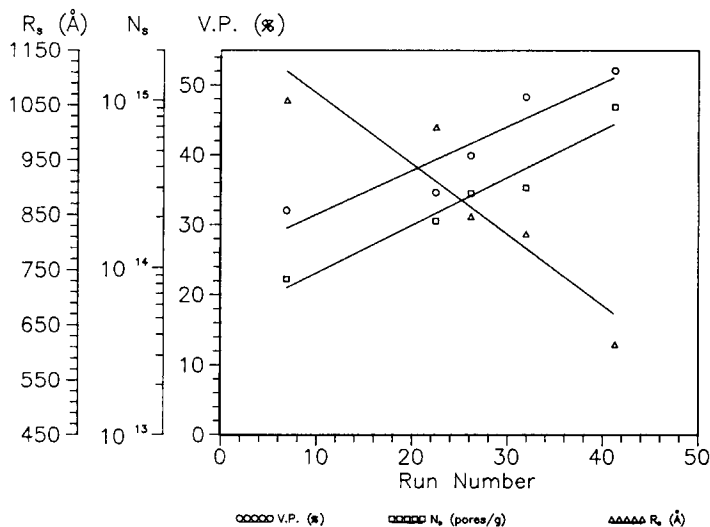
Figure 8 Relation between structural parameters of the PAC/AS blend fibers and run number of the AS copolymers. R_s: the radius of spherical pores; N_s: the number of the pores.

in porous blend acrylic fibers, its very low mercury density and high void proportion tend to affirm that in its structure there must be present many void spaces. These might exist very possibly in two forms: One acts as a system of capillaries connecting the pores in the interior of the fiber with its exterior environments and the other lies in the interphase regions of the two polymers in the blend. The electron micrographs are shown in Figures 1 and 5. In Figure 5 the copolymer is attacked by the butanone used as a treating medium, leaving pores behind. This leads us to believe that the interphase region might be looser or even more porous than the in-

terior of the polymer phases. In the interphase region two kinds of macromolecules must naturally interpenetrate each other. Some macromolecules of copolymer 2 might even penetrate into polymer 1, making the structure of the PAC phase more amorphous and forming in it a great number of capillary channels that are far richer in blends than in regular PAC fibers.

If the styrene content is low, the copolymer particles are dispersed finely, while on the contrary,
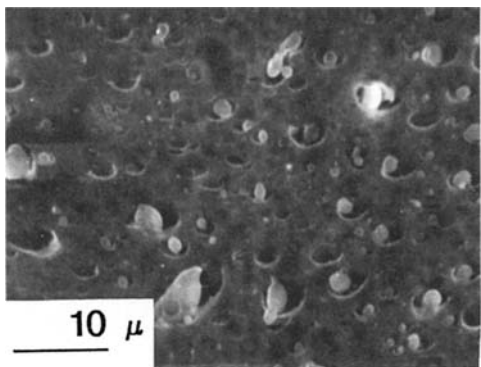

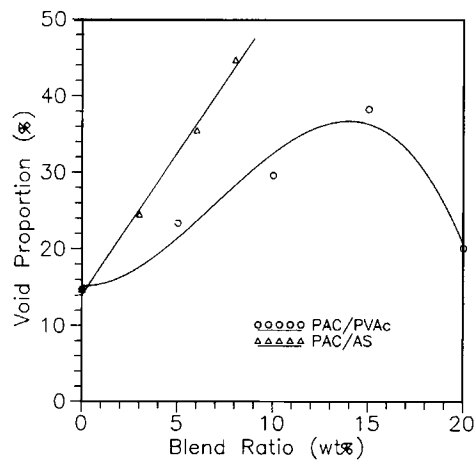**Figure 9** Electron micrograph of PAC/AS (90/10) film coagulated in water at 10°C.

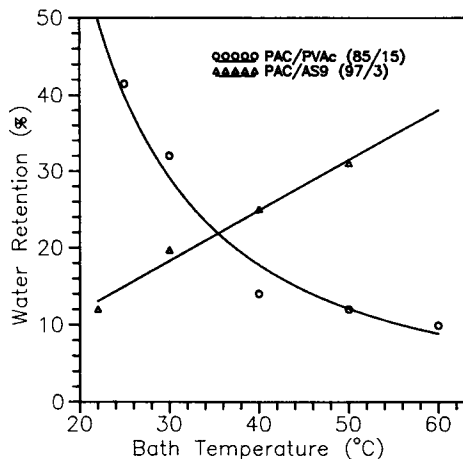**Figure 10** Effect of blend ratio on water retention of the blend fibers.

Figure 11   Effect of spin bath temperature on water retention of the blend fibers.

Figure 13   The void size distribution in PAC/PVAc (85/15) blend fibers.

high styrene content in the copolymer might result in coarser dispersion. These can be observed from the phase contrast micrograph given in Figures 2 and 3. With still further increase of styrene content much beyond 50%, phase separation may result in droplets that are less efficient in producing void spaces. This is illustrated by the data shown in Figure 7 given before.

Figure 9 is another electron micrograph that shows clearly the morphological structure of a blend acrylic film, PAC/AS (90/10), a minor copolymer being present as the isolated phase. The interphase region as a site of void spaces seems to be quite evident.

Formation Processes Controlling Voids Production

Blend Ratio

The phase separation properties will depend not only on the composition of the copolymer but also on the blend ratio of polymers 1 and 2. There seems to be a limit to the increase of interfacial energy between the two phases formed by the two polymers; with increase of blend ratio of polymer 2 to polymer 1, a maximum will soon be reached when the blend ratio attains 15%, after which the interfacial area will drop rapidly. This is shown clearly in Figure 10 for PAC/PVAc blend. For PAC/AS blend the maximum was
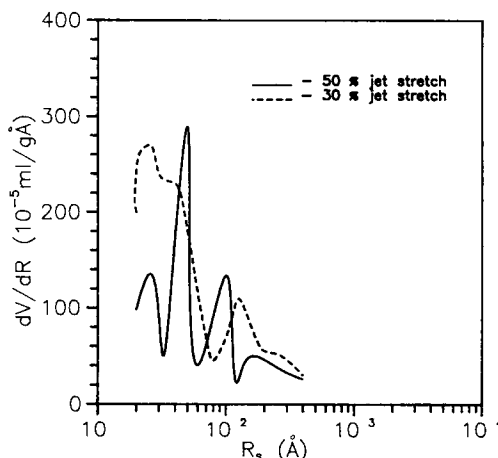

Figure 12   Effect of jet stretch on void proportion of the blend fibers.

Figure 14   The void size distribution in PAC/PVAc (85/15) blend fibers.
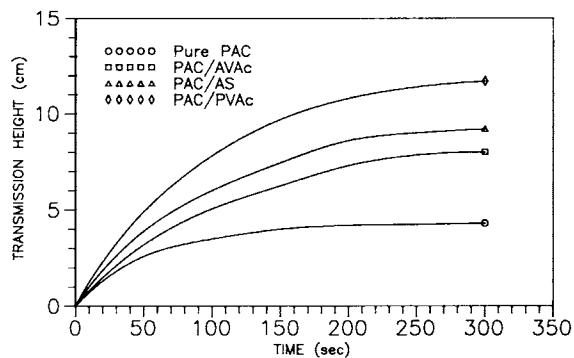
Figure 15 Capillary rise vs. time for ordinary and porous acrylic fibers.

not found, probably due to the range of variation of AS copolymer of 10% used in the test, which is not wide enough.

Effect of Temperature of Spinning on Void Production

Figure 11 shows the effect of the coagulation bath temperature on the void structure of the blend acrylic fiber. The opposite effects of coagulation temperature on the water retention value of PAC/ PVAc and PAC/AS was clearly shown. The cause of this difference might possibly be traced to the difference in the glass transition temperature of the copolymers PVAc and AS; the former possesses a glass transition temperature that lies in the range 20–60°C (the coagulating bath temperature we used), while the latter has a glass transition temperature much higher than that of the coagulating bath. The mechanism is not wholly elucidated yet.
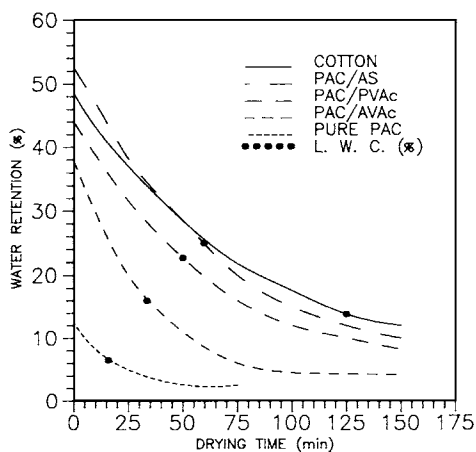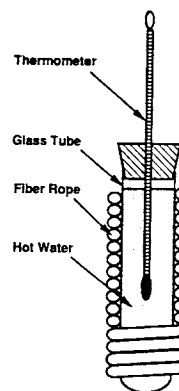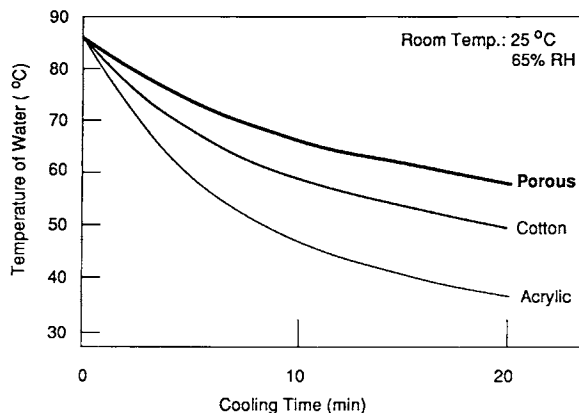

Figure 16 Rate of drying of various fibers (15°C, 60%RH).

Figure 17 Thermal insulating properties of various fibers (25°C, 65%RH) with a diagram of testing device.

Effect of Jet Stretch

Jet stretch will enhance void proportion due to fracture upon high degree of stretching. This phenomenon is also shown in Figure 12. Also the dispersed particles can be drawn into cylindrical shape by stretching. The effect of jet stretch on pore size and its distribution will be given later in connection with properties of porous acrylic fibers.

Properties of Porous Acrylic Blend Fibers

The following are the most valuable properties of the copolymer blend acrylic fibers:

Voids and Void Size Distribution

The voids and their distribution can be measured by mercury porosimetry.[8] The effects of temperature and jet stretch on void distribution are shown in Figures 13 and 14. It should be noted that the results

here obtained bear the same sense as those given in Figures 11 and 12, although the voids expressed as water retention and void proportion in these figures are different from that measured by mercury porosimetry as shown in Figures 13 and 14, the latter being those for finer ones present in the void structure.

Capillary Rise

A strand of porous acrylic blend fiber, held vertically over a beaker of water with its lower end inserted beneath the water surface, will possess a wicking action, causing the water to rise along the fiber strand. Such phenomenon is usually termed "capillary rise." Such results as shown in Figure 15. They represent the capillary absorption power of the material.

Drying of Water Releasing Property

While porous acrylic blend fiber can absorb water very quickly from a liquid source, it can also release its absorbed water rapidly by giving it to a drying
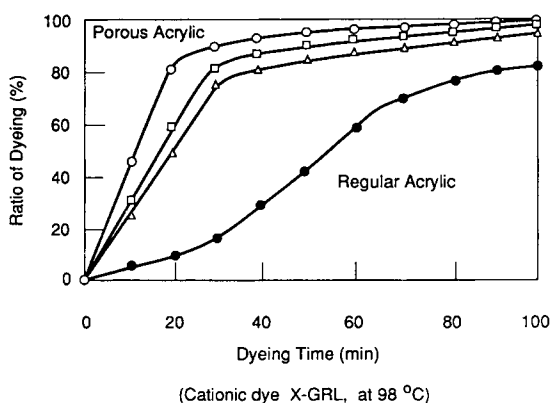

(Cationic dye X-GRL, at 98 °C)

Porous Acrylic   Regular Acrylic

Figure 18   Dyeing curves and cross sections of regular and porous acrylic fibers.

atmosphere. There is an important property, called the limiting water content (LWC) that is the threshold water content of a cloth giving the sensation of dampness to its wearer. This is shown as dots in Figure 16, which are the rate of drying curves of various acrylic blend fibers, together with a rate of drying curve for cotton, for comparison. From these, it is quite evident that most porous acrylic blend fibers are superior to cotton in WR and LWC values.

Thermal Insulating Properties

In this respect porous acrylic blend fibers show somewhat better thermal insulating properties to cotton, apparently due to their high void content, as shown in Figure 17.

Dyeing Properties

The rates of dyeing curve of PAC and three PAC blend fibers are shown in Figure 18. Not only is the rate of dyeing of blend fiber higher than regular PAC fiber, but also their equilibrium dyestuff take-ups are high, probably due to the presence of both voids and copolymer.

REFERENCES

1. Asahi Chemical Industry Co. Ltd., *Japan Kokai*, 52-107325 (1977), 52-114725 (1977), 54-68415 (1979).
2. T. Fukui and T. Sekiguchi, *Sen-I Gakkaishi*, **36**(8), 313 (1980).
3. P. Lennox-Kerr, *Text. Inst. Ind.*, **19**(3), 83 (1981).
4. G. Komatsu and S. Bukyo, *Jpn. Res. Assn. Text. End-Uses*, **23**(9), 359 (1982).
5. A. Zhang, *Synthetic Fibers*, **4**, 9 (1980).
6. R. L. Scott, *J. Polym. Sci.*, **9**, 423 (1952).
7. N. Oi and K. Miyazaki, *Kobunshi Kagaku*, **29**, 388 (1972).
8. J. Qin, Z. Liu, M. Yang, P. Mao, and F. Li, *Text. Res. J.*, **57**(8), 433 (1987).